Journal Name

COMMUNICATION

Iron Chelators Inhibit the Heme-Degradation Reaction by HutZ from *Vibrio cholerae*

Received 00th January 20xx,
Accepted 00th January 20xx

DOI: 10.1039/x0xx00000x

www.rsc.org/

Nobuhiko Dojun,[a] Yukari Sekine,[a] Koichiro Ishimori,[a,b] and Takeshi Uchida*[a,b]

HutZ is a heme-degrading enzyme. We found that the heme-degradation reaction by HutZ is inhibited by the iron chelators. Kinetic analysis of each heme-degradation step suggest that water molecules hydrogen bonded to Thr27 are involved in proton transfer to Fe(III)-OO$^-$, and that this step is inhibited by iron chelators.

The acquisition of iron is essential for survival, growth, and virulence of bacterial pathogens. Pathogenic bacteria acquire iron through iron-siderophore and heme protein scavenging systems. *Vibrio cholerae*, a Gram-negative bacteria, is the causative agent of cholera[1,2]. The genome sequence of *V. cholerae* and bioinformatics-based analyses predict the presence of putative genes encoding proteins termed Hut (Heme utilization) for heme acquisition[3,4]. We previously found that one of these Hut proteins, HutZ, degrades heme to β- or δ-biliverdin in vitro[5]. To quantify the iron released from heme by degradation, we added ferrozine, which forms a stable complex with iron, to a reaction solution containing heme-HutZ and ascorbic acid. We serendipitously found that the reaction proceeded very slowly in the presence of ferrozine. This result indicates that iron chelators can inhibit the heme-degradation reaction of HutZ. Thus, in the current study, we investigated the mechanism by which iron chelators inhibit heme degradation.

As shown in Fig. 1, which presents spectral changes following addition of ascorbic acid to ferric heme-HutZ, ascorbic acid caused a decrease in the Soret band at 406 nm, attributable to heme breakdown (Fig. 1A), as previously reported[5]. Addition of ferrozine 60 min after the reaction resulted in the appearance of a new band at 562 nm that reflects formation of a ferrozine-iron complex[6]. The heme-degradation ratio, defined as the ratio of iron concentration

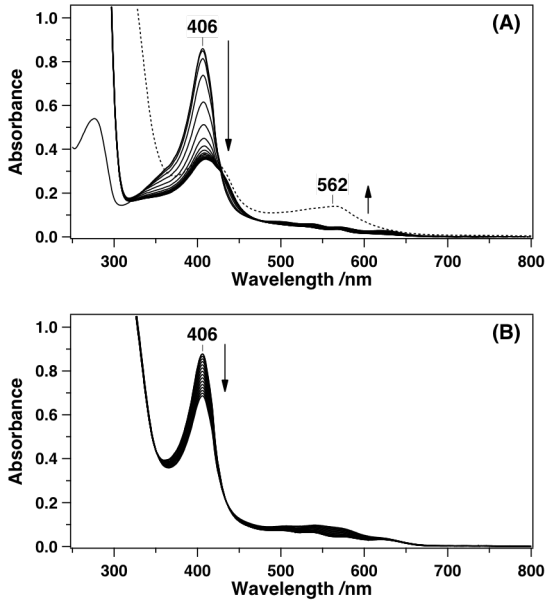

Fig. 1 Heme-degradation reaction of the heme-HutZ complex with ascorbic acid (1.0 mM) in 50 mM MES-OH/150 mM NaCl (pH 6.0) at 25 °C. To prevent nonenzymatic coupled oxidation, approximately 1 μM catalase was included (ε_{405} = 420 mM^{-1} cm^{-1} for the tetramer[25]). Spectra were measured before addition of ascorbic acid and at 8-min intervals for 56 min after the addition of ascorbic acid. Ferrozine (0.10 mM) was added (A) 30 min after the reaction or (B) before the reaction. Dotted line in (A) is the spectrum obtained following addition of ferrozine 60 min after initiation of the reaction.

captured by ferrozine to the initial heme concentration, was 86% (Table S1†). The most of the remaining absorbance at 406 nm originates from catalase. By contrast, addition of ferrozine prior to the reaction caused little decrease in the Soret band (Fig. 1B), suggesting that the heme-degradation reaction is repressed by ferrozine (Table S1†). This change was not caused by pH change upon addition on ferrozine to the solution and irreversible.

To determine whether inhibition of heme degradation by ferrozine requires the iron-chelating property of ferrozine or a specific interaction of ferrozine with HutZ, we monitored the same reaction in the presence of the typical iron chelators, EDTA, citric acid, and deferoxamine (DFO). Although EDTA did

[a] *Graduate School of Chemical Sciences and Engineering, Hokkaido University, Sapporo 060-8628, Japan*
[b] *Department of Chemistry, Faculty of Science, Hokkaido University, Sapporo 060-0810, Japan. E-mail: uchida@sci.hokudai.ac.jp*

†Electronic Supplementary Information (ESI) available: Materials and methods, and supplementary figures. See DOI: 10.1039/x0xx00000x

not affect the heme-degradation reaction, DFO and citric acid, in addition to ferrozine, significantly slowed the reaction (Fig. S1†). The dependence of this inhibition on the concentration of citric acid, ferrozine, and DFO was investigated. Fig. 2 shows the relative intensity ratio of the absorbance at 406 nm at 30 min after the reaction to the initial absorbance, where larger values indicate greater inhibition. The addition of chelators increased this ratio, indicating that the amount of heme degradation was decreased with increasing chelator concentration. The inhibition constant (K_i) for DFO was 5.7 μM, which is smaller than that for ferrozine (52 μM) and citric acid (6.0×10^2 μM) (Fig. 2). The stability constant (K_M) of ferrous iron for DFO (~10^{10} M)[7] is higher than that of citric acid ($10^{4.6}$ M)[8], but smaller than that of ferrozine ($10^{15.6}$ M)[9]. These results indicate that the inhibition mechanism of iron chelators does not necessarily involve metal chelation.

The deceleration of the enzymatic reaction of HutZ by iron chelators raised the possibility that the chelators affect the structure of the active site of heme-HutZ. To test this, we measured UV-vis absorption and resonance Raman spectra of heme-HutZ. The Soret maximum of ferric heme-HutZ at 406 nm remained after the addition of DFO (Fig. S2A†). Moreover, resonance Raman spectra of the CO-heme complex of HutZ revealed that the addition of DFO did not shift Fe-CO ($\nu_{Fe\text{-}CO}$) or C-O ($\nu_{C\text{-}O}$) stretching modes from their original values of 506 cm^{-1} and 1933 cm^{-1}, respectively, measured in the absence of chelators (Fig. S2B†). We also measured circular dichroism spectra of heme-HutZ to determine whether the addition of DFO caused any secondary structural changes. The ellipticity at 222 nm, which represents the α-helical structure, was virtually insensitive to DFO (Fig. S2C†), although that below 215 nm was slightly decreased in the presence of DFO. This latter change likely reflects the absorption of DFO itself, which exhibits a broad band between 200 and 240 nm (Fig. S2D†). These results suggest that DFO does not induce a detectable change in secondary structure. Thus, we postulated that the chelators do not bind to heme-HutZ and disturb its active site. To confirm this, we applied isothermal titration calorimetry to study the energetics of chelator binding to heme-HutZ. Indeed, no binding heat was detected for a solution of DFO and heme-HutZ (Fig. S3†), indicating that DFO does not likely bind HutZ directly.

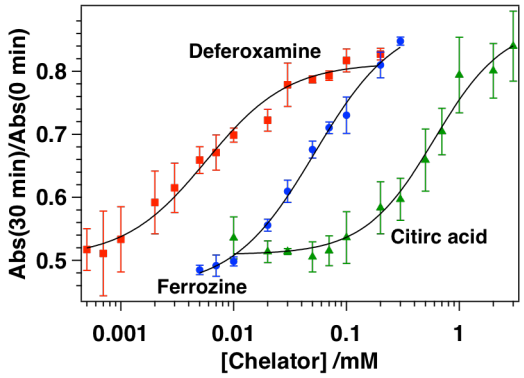

Fig. 2 Changes in absorbance at 406 nm during heme degradation by HutZ in the presence of DFO, citric acid, or ferrozine. The data points in UV-vis spectra were obtained before addition of ascorbic acid (1 mM) and 30 min after addition. Abs(30 min)/Abs(0 min) values are plotted against iron chelator concentration, and the data were fit to the Hill equation.

To clarify how chelators cause inhibition, we focused on the heme-degradation mechanism of HutZ, which is a multistep reaction, as shown in Fig. S4†[5,10,11]. Accordingly, we next sought to determine which step is inhibited by the chelators. First, we measured the reduction rate of heme, k_1, the first step of heme degradation (Fig. S4†). Fig. S5† shows the time course of absorption changes after the addition of ascorbic acid to ferric heme-HutZ, in the presence of CO to prevent oxidation to ferric heme. Upon reduction, the Soret maximum at 406 nm underwent a red shift to 418 nm—the same position of the Soret band in CO-bound heme[5]. The time course of absorbance changes at 418 nm in the absence of DFO was fit to a single exponential, which yielded a k_1 of 0.052 ± 0.005 min^{-1}. In the presence of DFO, the k_1 was 0.045 ± 0.008 min^{-1}, showing that DFO does not affect this step.

The second step in heme degradation is O_2 binding to ferrous heme (Fig. S4†). It is difficult to obtain the rate constant for this step (k_2), because O_2-bound heme-HutZ is rapidly autoxidized to ferric heme[5], or converted to hydroperoxy heme, leading to degradation of heme. Therefore, we measured the cyanide (CN) ion-binding rate (k_2') instead of k_2. A typical time course for the reaction of heme-HutZ with CN using a stopped-flow apparatus is shown in Fig. S6A†. Under conditions of excess of CN, a pseudo-first rate constant (k_{obs}) was obtained from the single-exponential fit. The obtained k_{obs} values increased linearly with increasing concentrations of CN (Fig. S6B†). The second-order rate constant, k_2', obtained from the slope of this relation, was 0.88 ± 0.01 $mM^{-1}s^{-1}$ in the absence of DFO and only slightly smaller (0.76 ± 0.01 $mM^{-1}s^{-1}$) in the presence of DFO. Therefore, the step involving ligand binding to heme is unlikely to be inhibited by DFO. Finally, the rate constant for the formation of verdoheme, k_4 (Fig. S4†), was compared. In the reaction with H_2O_2, the Soret band disappeared with a concomitant increase in a band at 644 nm[5] (Fig. S7†). The value of k_4 obtained by fitting the data at 644 nm to a single exponential curve, was 0.38 s^{-1}, which is approximately equal to that in the presence of DFO (0.39 s^{-1}).

As described above, the rates for heme reduction (k_1), ligand binding (k_2), and verdoheme formation (k_4) were unaffected by the addition of iron chelators. The remaining step is conversion of oxyheme to hydroperoxy heme, with a rate constant of k_3 (Fig. S4†). However, it is difficult to directly measure k_3 owing to the extremely short lifetime of hydroperoxy heme. This step is divided into two steps: the one-electron reduction of oxyheme to Fe(III)-OO^-, and protonation of Fe(III)-OO^- to hydroperoxy heme. Considering that the addition of DFO does not change k_1, it would also not alter the redox potential of heme-HutZ, indicating that the rate of one-electron reduction of oxyheme would not be affected. Thus, we postulated that DFO inhibits the second step: protonation of Fe(III)-OO^-.

In mammalian heme oxygenase (HO), X-ray crystal structure and other biochemical and biophysical studies suggest that protonation of oxyheme is mediated by distal water molecules, which serve as proton sources (Fig. S8†)[11–13].

However, it is not clear whether HutZ also contains such water molecules in the active site. To investigate whether water molecules are needed for hydroxylation of oxyheme, we monitored the heme-degradation reaction in D_2O buffer. The time courses of absorbance changes at 406 nm in reactions with ascorbic acid in H_2O and D_2O buffer are illustrated in Fig. S9†. The relative absorption at 406 nm for D_2O 30 min after initiation of the reaction was higher than that of H_2O, implying that heme degradation in D_2O is slower than that in H_2O, suggesting that water molecules are involved in the process of proton transfer to Fe(III)-OO^-, as observed in HO[14–16].

This isotope effect on heme-degradation by HutZ suggests that a proton source is required for protonation of the Fe(III)-OO^- species. In HO-1, the terminal oxygen atom of the heme-bound O_2 interacts with a water molecule, which is stabilized by Asp140 (Fig. S8†)[17,18]. Replacement of Asp140 with alanine substantially suppresses proton transfer to Fe(III)-OO^- in HO-1 because of displacement and/or fluctuations of the water molecules[19–21]. The distal Asp140 allows water molecules in the distal pocket to interact with heme-bound O_2[20,22]. Although the heme complex of HutZ has not been crystallized, the crystal structure of a homologous protein, HugZ, from *Helicobacter pylori* suggests that Thr27 of HutZ is present in the active site (Fig. S10†)[23]. Thus, we predicted that Thr27 plays a role in protonation of Fe(III)-OO^- analogous to that of Asp140 in HO-1. To investigate whether the hydroxyl group at position 27 is essential for protonation of the iron-bound O_2, we replaced Thr27 with valine or serine, and examined the heme-degradation activity of the resulting mutants. The time course of the decrease in the Soret band revealed that the heme-degradation rate was significantly slower for the heme-HutZ T27V mutant than for heme-HutZ wild-type (WT) (Fig. 3). In addition, mutation of Thr27 to valine caused a 2-fold decrease in the amount of liberated ferrous iron (Table S1†). To investigate the step inhibited in the T27V mutant, we measured the rate constants for heme-degradation (Fig. S4†). The values for k_1, k_2, and k_4 for the heme-HutZ T27V mutant were almost the same as those for heme-HutZ WT (Table S2†). In contrast, for the T27S mutant, in which the hydroxyl group at position 27 is retained, the heme-degradation rate and amount of iron released from heme were almost identical to those of heme-HutZ WT (Fig. 3, Table S1†). These results suggest that the OH group of Thr27 is involved in protonation of Fe(III)-OO^-.

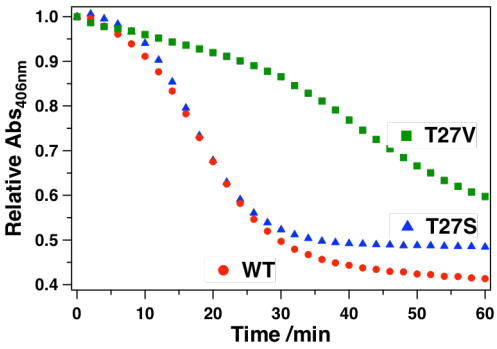

Fig. 3 Changes in absorbance intensity at 406 nm in reactions of heme-HutZ WT, and heme-HutZ T27V and T27S mutants with ascorbic acid (1 mM).

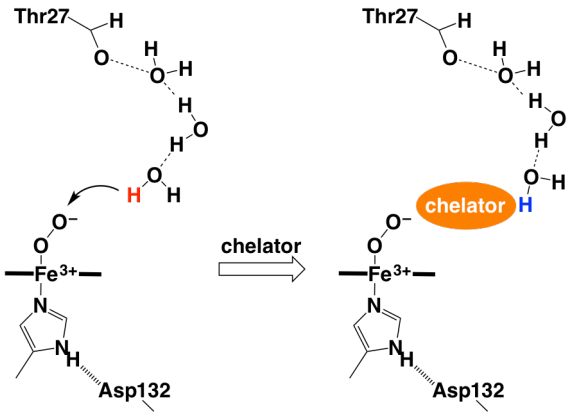

Fig. 4 Proposed mechanism for inhibition of heme degradation reaction by iron chelators.

These observations indicate that iron chelation perturbs proton transfer from water molecules to Fe(III)-OO^-, and Thr27 contributes to the presence of water molecules in the active site. A proposed mechanism for inhibition by iron chelators is illustrated in Fig. 4. According to this model, iron chelators inhibit the heme-degradation reaction by perturbing localization of the proton source—water molecules—making it difficult for HutZ to form the Fe(III)-OOH species. The exothermic heat of interaction of DFO with distal water molecules would be canceled by the endothermic heat of disruption of the interaction with bulk water molecules (Fig. S3†).

Inhibition of HutZ by iron chelators prompted us to investigate the possibility of antibiotics as inhibitor of HutZ, because tetracycline, which is the most effect current treatments for cholera, is an inhibitor of protein synthesis as well as an iron chelator[24]. Thus, we speculated that

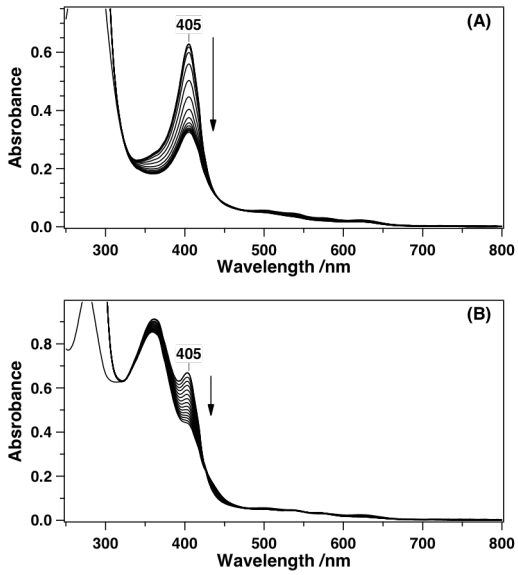

Fig. 5 Heme-degradation reaction of the heme-HutZ complex with ascorbic acid (1.0 mM) at pH 6.0 (A) in the presence of 50 mM chloramphenicol and (B) 50 mM tetracycline. Spectra were measured before addition of ascorbic acid and at 8-min intervals for 56 min after addition of ascorbic acid. Tetracycline caused a large absorption below 400 nm.

tetracycline also affects the heme-degradation activity of HutZ. The spectral changes that follow addition of ascorbic acid in the presence of antibiotics are shown in Fig. 5. In the presence of chloramphenicol, a representative antibiotic, heme was degraded by HutZ (Fig. 5A). In contrast, the Soret band diminished very little in the presence of tetracycline (Fig. 5B), indicating that the heme-degradation reaction was repressed, similar to that observed in the presence of DFO. These observations support the conclusion that substrates possessing iron-chelating ability could be possible treatments for cholera.

In summary, we found that iron chelators are able to inhibit the heme-degradation reaction of HutZ by perturbing proton transfer to Fe(III)-OO^- from water molecules in the distal cavity. This mechanism suggests that iron chelators are candidate antibiotics for use against *V. cholerae*.

This study was supported in part by a Grant-in-Aid for Scientific Research (16K05835 to T.U., 13J04076 to Y.S., and 15H00909 to K.I.) from the Ministry of Culture, Education, Sports, Science, and Technology of Japan. We thank Prof. Yoshikazu Tanaka for ITC measurement.

Notes and references

1 J. B. Kaper, J. G. Morris and M. M. Levine, *Clin. Microbiol. Rev.*, 1995, **8**, 48–86.
2 S. M. Faruque, M. J. Albert and J. J. Mekalanos, *Microbiol. Mol. Biol. Rev.*, 1998, **62**, 1301–1314.
3 E. E. Wyckoff, M. Schmitt, A. Wilks and S. M. Payne, *J. Bacteriol.*, 2004, **186**, 4142–4151.
4 E. E. Wyckoff, A. R. Mey and S. M. Payne, *Biometals*, 2007, **20**, 405–416.
5 T. Uchida, Y. Sekine, T. Matsui, M. Ikeda-Saito and K. Ishimori, *Chem. Commun.*, 2012, **48**, 6741–6743.
6 L. L. Stookey, *Anal. Chem.*, 1970, **42**, 779–781.
7 H. Keberle, *Ann. N. Y. Acad. Sci.*, 1964, **119**, 758–768.
8 U. Rauen, A. Springer, D. Weisheit, F. Petrat, H.-G. Korth, H. de Groot and R. Sustmann, *ChemBioChem*, 2007, **8**, 341–352.
9 C. Gibbs, *Anal. Chem.*, 1976, **48**, 1197–1201.
10 P. R. Ortiz de Montellano, *Curr. Opin. Chem. Biol.*, 2000, **4**, 221–227.
11 M. Unno, T. Matsui and M. Ikeda-Saito, *Nat. Prod. Rep.*, 2007, **24**, 553–570.
12 M. Sugishima, K. Moffat and M. Noguchi, *Biochemistry*, 2012, **51**, 8554–8562.
13 H. Chen, Y. Moreau, E. Derat and S. Shaik, *J. Am. Chem. Soc.*, 2008, **130**, 1953–1965.
14 S. Hallén and T. Nilsson, *Biochemistry*, 1992, **31**, 11853–11859.
15 J. Aikens and S. G. Sligar, *J. Am. Chem. Soc.*, 1994, **116**, 1143–1144.
16 R. Davydov, T. Matsui, H. Fujii, M. Ikeda-Saito and B. M. Hoffman, *J. Am. Chem. Soc.*, 2003, **125**, 16208–16209.
17 D. J. Schuller, A. Wilks, P. R. Ortiz de Montellano and T. L. Poulos, *Nat. Struct. Biol.*, 1999, **6**, 860–867.
18 M. Sugishima, Y. Omata, Y. Kakuta, H. Sakamoto, M. Noguchi and K. Fukuyama, *FEBS Lett.*, 2000, **471**, 61–66.
19 R. Davydov, V. Kofman, H. Fujii, T. Yoshida, M. Ikeda-Saito and B. M. Hoffman, *J. Am. Chem. Soc.*, 2002, **124**, 1798–1808.
20 H. Fujii, X. Zhang, T. Tomita, M. Ikeda-Saito and T. Yoshida, *J. Am. Chem. Soc.*, 2001, **123**, 6475–6484.
21 L. K. Lightning, H. W. Huang, P. Moënne-Loccoz, T. M. Loehr, D. J. Schuller, T. L. Poulos and P. R. Ortiz de Montellano, *J. Biol. Chem.*, 2001, **276**, 10612–10619.
22 L. Lad, J. Wang, H. Li, J. Friedman, B. Bhaskar, P. R. Ortiz de Montellano and T. L. Poulos, *J. Mol. Biol.*, 2003, **330**, 527–538.
23 Y. Hu, F. Jiang, Y. Guo, X. Shen, Y. Zhang, R. Zhang, G. Guo, X. Mao, Q. Zou and D.-C. Wang, *J. Biol. Chem.*, 2011, **286**, 1537–1544.
24 A. Albert and C. W. Rees, *Nature*, 1956, **177**, 433–434.
25 T. J. Reid III, M. R. N. Murthy, A. Sicignano, N. Tanaka, W. D. L. Musick and M. G. Rossmann, *Proc. Natl. Acad. Sci.*, 1981, **78**, 4767–4771.

